THE ROYAL SOCIETY

Published online 28 February 2002

Fibrillin: from microfibril assembly to biomechanical function

Cay M. Kielty[1*], Clair Baldock[2], David Lee[2], Matthew J. Rock[2], Jane L. Ashworth[1] and C. Adrian Shuttleworth[2]

[1]*School of Medicine and* [2]*School of Biological Sciences, University of Manchester, Manchester M13 9PT, UK*

Fibrillins form the structural framework of a unique and essential class of extracellular microfibrils that endow dynamic connective tissues with long-range elasticity. Their biological importance is emphasized by the linkage of fibrillin mutations to Marfan syndrome and related connective tissue disorders, which are associated with severe cardiovascular, ocular and skeletal defects. These microfibrils have a complex ultrastructure and it has proved a major challenge both to define their structural organization and to relate it to their biological function. However, new approaches have at last begun to reveal important insights into their molecular assembly, structural organization and biomechanical properties. This paper describes the current understanding of the molecular assembly of fibrillin molecules, the alignment of fibrillin molecules within microfibrils and the unique elastomeric properties of microfibrils.

Keywords: fibrillin assembly; microfibrils; extensibility; organization

1. INTRODUCTION

Fibrillin-rich microfibrils are thin, filamentous, connective tissue assemblies present in virtually all dynamic connective tissues (figure 1) (Kielty & Shuttleworth 1995; Handford *et al.* 2000; Sherratt *et al.* 2000). In elastic tissues, such as aorta, lung, skin and elastic cartilage, preformed bundles of microfibrils form a template for tropoelastin deposition during elastic fibre formation and are retained as an outer mantle of mature elastic fibres (Mecham & Heuser 1991). Microfibril arrays are often abundant in tissues that do not express elastin, such as the ciliary zonules of the eye, which hold the lens in dynamic equilibrium (Ashworth *et al.* 2000).

Several recent studies, based on whole tissues and on isolated fibrillin-rich microfibrils, have highlighted their unique elastic properties, which are critical to their biological function both when they act alone or in association with elastin. The extensibility of lobster aorta was accounted for by microfibril arrays that intersperse medial smooth muscle cells (McConnell *et al.* 1996). Extracted sea cucumber microfibrils exhibited long-range elastomeric properties (Thurmond & Trotter 1996). X-ray diffraction, tensile testing and stress–relaxation tests demonstrated that hydrated mammalian ciliary zonules and microfibril bundles are reversibly extensible in the presence or absence of calcium (Wess *et al.* 1998*a*; Wright *et al.* 1999). Isolated human microfibrils, entangled in debris during preparation for electron microscopy, can become stretched to periodicities of up to *ca.*165 nm (Keene *et al.* 1991). Extended microfibrils, often observed in matrix metalloproteinase-treated preparations, may reflect a pathological loss of elastic recoil (Ashworth *et al.* 1999*a*).

Early microscopy studies highlighted some distinctive staining characteristics of microfibrils that indicated a strongly anionic nature (Cleary & Gibson 1983). Rotary shadowing and negative staining, extensively used to examine isolated microfibrils, have since revealed a 'beads-on-a-string' arrangement with an average periodicity of *ca.* 56 nm and apparent diameter of 10–14 nm (figure 2) (Wright & Mayne 1988; Fleischmajer *et al.* 1991; Keene *et al.* 1991; Kielty *et al.* 1991; Ren *et al.* 1991; Wallace *et al.* 1991). STEM analysis of the microfibril mass and its axial distribution has revealed that beads correspond to mass peaks, whilst interbeads comprise a mass shoulder to one side of the bead, then a trough (Sherratt *et al.* 1997). The molecular composition of this class of microfibrils remained unresolved until approximately 15 years ago, when antibodies raised to a human amnion extract were found to label the microfibrils and to recognize a novel glycoprotein, designated fibrillin (Sakai *et al.* 1986). Molecular cloning studies rapidly followed and it soon became clear that there were two highly homologous isoforms, fibrillin-1 encoded by a gene on chromosome 15 and fibrillin-2 encoded by a gene on chromosome 5 (Lee *et al.* 1991; Maslen *et al.* 1991; Pereira *et al.* 1993; Zhang *et al.* 1994). Linkage of mutations in the gene encoding fibrillin-1 to Marfan syndrome, and in the gene encoding fibrillin-2 to the related disorder congenital contractural arachnodactyly, confirmed both the key role of fibrillins in microfibril formation and the importance of microfibrils to connective tissue integrity (Robinson & Godfrey 2000). Numerous biochemical and antibody mapping studies have since confirmed that fibrillin molecules do, indeed, assemble to form the microfibril scaffold.

Both fibrillin isoforms are large glycoproteins (*ca.* 350 kDa) with multidomain structures dominated by 43 calcium-binding consensus sequences (cbEGF domains; figure 3*a*; Pereira *et al.* (1993); Zhang *et al.* (1994); Down-

* Author for correspondence (cay.kielty@man.ac.uk).

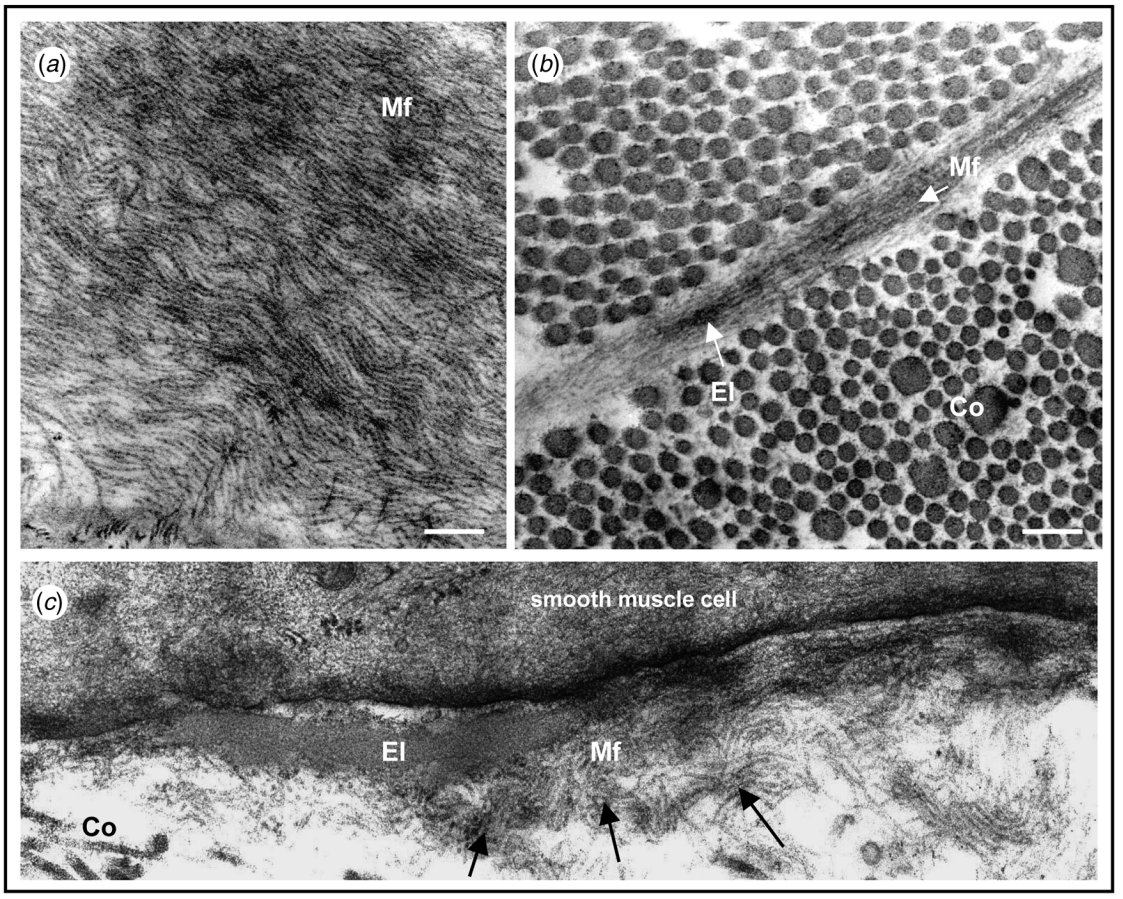

Figure 1. Vertebrate and invertebrate fibrillin-rich microfibrils. (*a*) Ultrathin fixed section of a lobster aorta showing fibrillin-rich microfibrils in longitudinal section, after staining with uranyl acetate and lead citrate. (*b*) Ultrathin fixed section of a murine skin biopsy stained with uranyl acetate and lead citrate. (*c*) Ultrathin section of murine aorta, showing an assembling elastic fibre adjacent to a smooth muscle cell. In (*b*) and (*c*), the microfibrillar mantle (Mf), elastin core (El) and transversely sectioned collagen fibrils (Co) are indicated. Scale bars, 400 nm.

ing *et al.* (1996)). These domains are interspersed with 8-cysteine domains, also known as TB modules because they are homologous to transforming growth factor β (TGF-β)-binding 8-cysteine-containing motifs found in latent TGF-β-binding proteins (Yuan *et al.* 1997; Sinha *et al.* 1998). Fibrillin-1 has a 58 amino acid proline-rich region towards the amino terminus, which may act as a 'hinge-like' region and which, in fibrillin-2, is replaced by a glycine-rich sequence. As predicted by the many cbEGF domains, fibrillin molecules bind calcium, which results in an extended rod-like conformation (Reinhardt *et al.* 1997). Ultrastructural and X-ray diffraction studies have shown that bound calcium profoundly influences the packing and periodicity of isolated microfibrils and hydrated microfibril arrays (Kielty & Shuttleworth 1993; Cardy and Handford 1998; Wess *et al.* 1998*a*)

The complexity of microfibrils is further enhanced by the fact that they are probably multicomponent polymers. However, their molecular composition remains poorly defined, both in terms of the relative contributions of the two fibrillin isoforms in different tissues and at different stages of development, and in respect of their interactions with other molecules. Immunohistochemical and biochemical studies have highlighted that a number of matrix molecules colocalize with microfibrils in various tissues; they include microfibril-associated glycoproteins (including microfibril-associated glycoprotein (MAGP) 1 and 2), latent transforming binding proteins and chondroitin sulphate proteoglycans (Kielty *et al.* 1996; Dallas *et al.* 2000; Trask *et al.* 2000*a*; Unsold *et al.* 2001). In addition, during elastic fibre formation, microfibrils interact with tropoelastin and are associated with lysyl oxidase and elastin (Trask *et al.* 2000*b*), as well as elastin–microfibril interface proteins such as emilin (Doliana *et al.* 1999) and fibulin-2 (Reinhardt *et al.* 1996*a*; Raghunath *et al.* 1999*a*). It is not known which, if any, of these microfibril-associated molecules are integral microfibril components, or indeed how their presence, or absence, may influence microfibril structure, extensibility and function.

Defining the assembly, molecular alignment and stabilization of fibrillin-rich microfibrils is central to understanding their structural properties and to resolving current controversies relating to their structure and function (figure 3). This review describes recent progress in determining how fibrillin molecules associate to form unique, extensible, beaded microfibrils and how fibrillin molecules are aligned and stabilized within microfibrils. This information now paves the way for determining the physiological periodic range of microfibril extensibility, the molecular basis of 'recoil' and how various forms of pathological insult may affect extensibility.

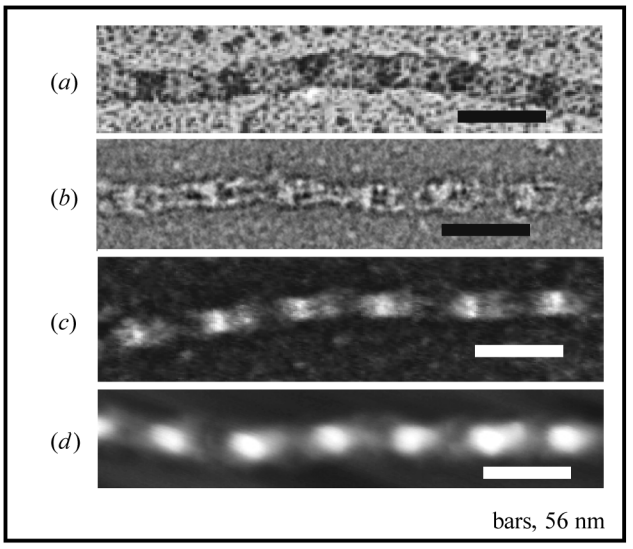

Figure 2. Ultrastructural appearance of isolated fibrillin-rich microfibrils. Isolated untensioned microfibrils have a 'beads-on-a-string' appearance and *ca.* 56 nm periodicity when visualized by a range of microscopy techniques. (*a*) TEM micrograph of a rotary shadowed microfibril. (*b*) TEM micrograph following negative staining. (*c*) STEM micrograph in the absence of staining or shadowing, showing microfibril mass. (*d*) Surface topography revealed by tapping mode atomic force microscopy. The beads and interbead regions are clearly visible using these ultrastructural approaches. Scale bars, 56 nm.

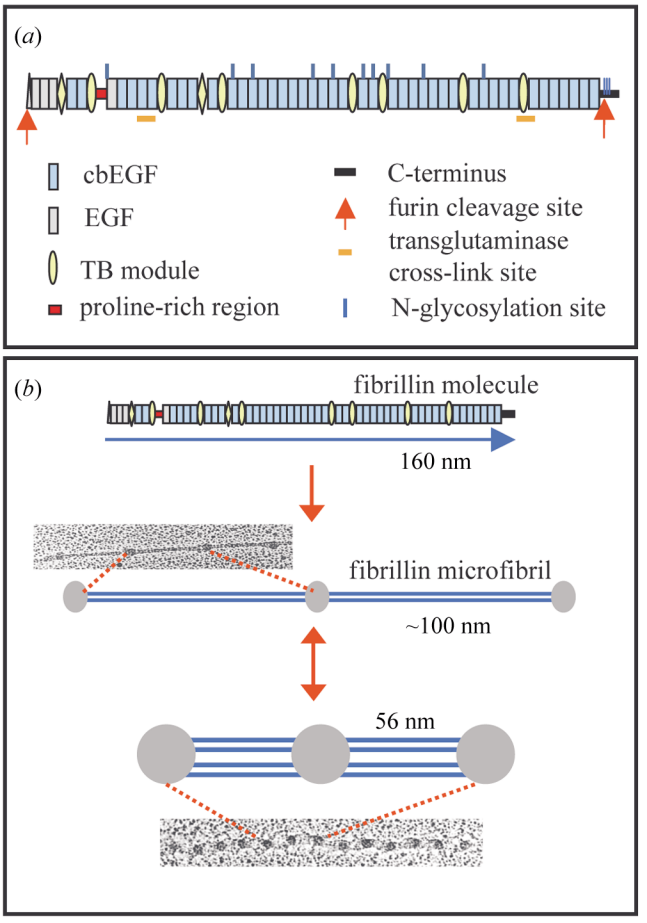

Figure 3. Schematic representation of the fibrillin-1 molecule and its assembly into extensible microfibrils. (*a*) Domain structure of fibrillin, highlighting how the contiguous arrays of cbEGF-like domains are interspersed with TB modules and the locations of the proline-rich region, N-glycosylation consensus sequences and putative transglutaminase cross-link sites. (*b*) Diagram highlighting how fibrillin-1 molecules (*ca.* 160 nm) assemble to form beaded microfibrils with variable periodicity (*ca.* 56–100 nm).

2. MOLECULAR ASSEMBLY

Many of the details of precisely how fibrillin molecules assemble into complex, extensible, beaded microfibrils still remain to be determined (figure 3*b*). The propensity of fibrillin molecules to form disulphide-bonded aggregates has hampered attempts to identify true intermediates of assembly. Moreover, conventional recombinant expression approaches to generate full-length fibrillin-1 molecules for *in vitro* assembly studies have, to date, proved ineffective. However, new recombinant approaches have at last begun to provide insights into the key fibrillin interactions that drive assembly, the defined intermediates of assembly and the role of processing in polymerization.

The N-terminal region of fibrillin-1 has been shown by several groups to readily aggregate *in vitro*, forming extensive disulphide-bonded aggregates (Ashworth *et al.* 1999*b*; Reinhardt *et al.* 2000). Specific N-terminal interactions are predicted to drive this aggregation that can then become stabilized with covalent disulphide linkages; an unpaired cysteine residue in the first hybrid TB-module has been implicated in intermolecular cross-linking (Reinhardt *et al.* 2000). Distinct, but overlapping, fibrillin N-terminal peptides have been shown, by two groups using different mammalian recombinant systems, to form dimers (figure 4*a*) (Ashworth *et al.* 1999*b*; Trask *et al.* 1999); however, it remains uncertain whether dimerization occurs intracellularly or upon secretion. We have now obtained the first direct evidence that recombinant full-length human fibrillin-1 rapidly forms dimers within the secretory pathway in a time-dependent manner (figure 4*b*) (Lee *et al.* 2001). These studies used an effective well-characterized *in vitro* transcription–translation system supplemented with semi-permeabilized cells, in which purified fibrillin-1 mRNA is translated as a [^{35}S]-cysteine-labelled protein that can readily and rapidly be monitored in SDS–PAGE and size fractionation studies. This system, which provided a powerful means of examining the fate of newly translocated fibrillin-1 molecules within the ER, has shown, for the first time, that full-length fibrillin-1 spontaneously formed disulphide-bonded dimers, then larger non-reducible intermediates in a time-dependent manner.

Cleavage sites for furin/PACE convertases are present close to the N- and C-termini of each isoform and C-terminal processing is known to be a prerequisite for extracellular deposition (Raghunath *et al.* 1999*b*; Ritty *et al.* 1999). Using the *in vitro* transcription–translation system with semi-permeabilized cells, it is now clear that the formation of fibrillin-1 dimers does not require furin treatment, although processing does accelerate the formation of larger aggregates (Lee *et al.* 2001). It is therefore tempting to speculate that furin processing is a prerequisite for extracellular linear accretion of dimers, or larger inter-

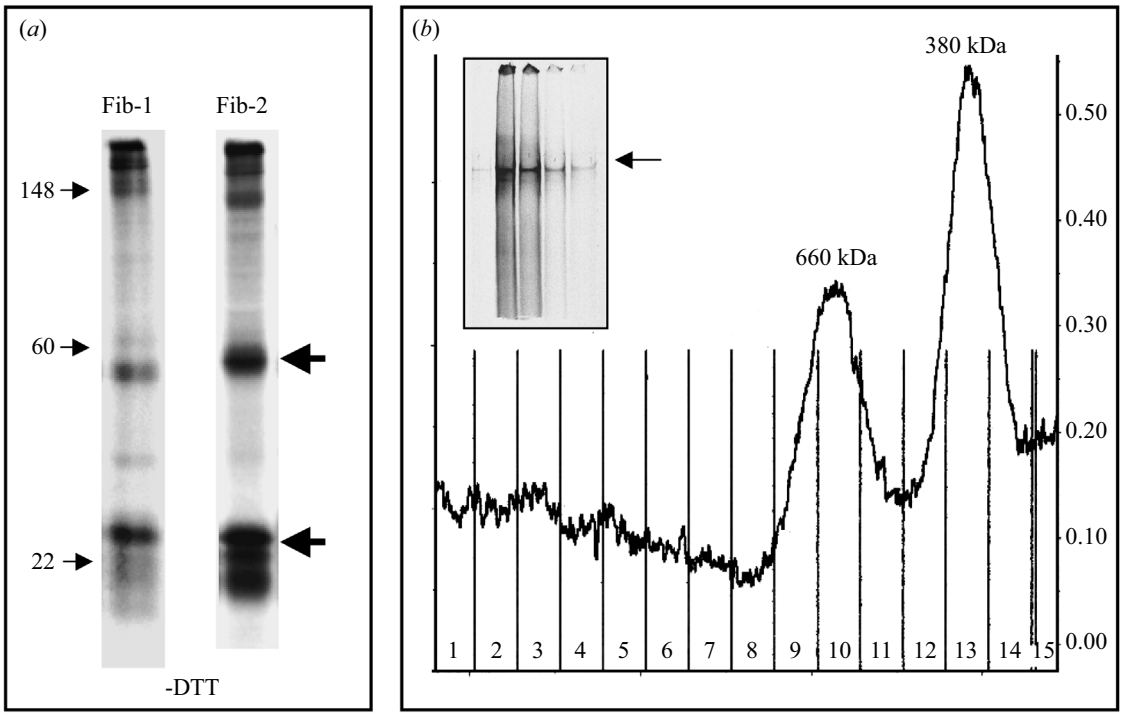

Figure 4. Fibrillin-1 dimer formation. (*a*) The proline-rich region and its flanking domains (exons 9–11) form dimers and higher assemblies. (*b*) The full-length fibrillin-1 molecule, purified by heparin affinity chromatography (see insert, SDS–PAGE in reducing conditions), resolves into monomers and dimers by size fractionation in native non-reducing conditions. The *x*-axis represents column fractions (volume) and the *y*-axis is optical density at 280 nm. These recombinant molecules were expressed in an *in vitro* transcription–translation system supplemented with semi-permeabilized cells as a source of secretory organelles (Ashworth *et al.* 1999*b*; Lee *et al.* 2001). Panel (*a*) is reproduced with permission from The Company of Biologists, UK.

mediates, to form microfibrils, in which case the location and regulation of processing must be crucial determinants of fibrillin assembly. A recent report suggests that a C-terminal fibrillin-1 heparin-binding site, activated upon processing, may be important in extracellular matrix deposition (Ritty *et al.* 2000). The precise pericellular location of these cleavage events remains controversial, although furins can be catalytically active within the *trans* Golgi and secretory vesicles. We have shown that the presence of N-linked carbohydrates within the C-terminus, and its association with calreticulin, can restrict processing (Ashworth *et al.* 1999*c*). The existence of mechanisms that can regulate furin processing emphasizes the crucial significance of this step for fibrillin assembly. However, the precise intracellular or extracellular location of processing and its consequences in terms of assembly and molecular interactions remain to be defined.

Dimers thus appear to be defined, disulphide-bonded intermediates of assembly and the fully assembled polymer is also stabilized by covalent cross-links, both disulphide bonds and transglutaminase-derived peptide linkages. Indeed, fibrillin-1 homotypic transglutaminase cross-links have been identified in peptides starting at residues 580 and 2312 (Qian & Glanville 1997). Tissue transglutaminase activity is probably an extracellular event that could stabilize newly assembled linear arrays of fibrillin. In our *in vitro* assembly studies, the presence of tissue transglutaminase activity rapidly generates fibrillin aggregates (Lee *et al.* 2001). Whether this reflects *in vivo* cross-linking events is unclear, but it is certain that fibrillin is an extremely attractive substrate for this enzyme. Thus, the physiological role of transglutaminase cross-linking in the assembly process and/or in the subsequent stabilization of microfibrils in different tissues, remains to be defined.

3. FIBRILLIN MOLECULE ALIGNMENT IN MICROFIBRILS

The intriguing, regular, beaded periodicity of microfibrils and detailed information on the molecular dimensions of fibrillin molecules has led to several proposed models of fibrillin alignment in microfibrils. A model based on antibody epitope mapping and measured molecular dimensions, suggested a parallel head-to-tail alignment of unstaggered fibrillin monomers with amino- and carboxy-termini at, or close to, the beads (Reinhardt *et al.* 1996*b*). STEM showed that isolated untensioned microfibrils have an asymmetric repeating bead–interbead organization, implying that microfibrils are directional and that fibrillin molecules are parallel (Sherratt *et al.* 1997). Staggered arrangements, based on extrapolation of molecular length from cbEGF-like domain dimensions and untensioned microfibril periodicity (approximately a one-half stagger) (Downing *et al.* 1996), or on alignment of the fibrillin-1 homotypic transglutaminase cross-links in an approximate one-third stagger, were also proposed (Qian & Glanville 1997). None of these models provides a molecular explanation for how assembled fibrillin forms extensible beaded microfibrils with variable periodicity, nor are they compatible with the axial mass distribution of untensioned microfibrils revealed by our STEM studies.

4. NEW MODEL OF FIBRILLIN ALIGNMENT IN EXTENSIBLE MICROFIBRILS

In an attempt to clarify outstanding anomalies in microfibril structure, we recently used AET to develop the first three-dimensional reconstructions of microfibrils (figure 5) (Baldock *et al.* 2001). We also localized fibrillin antibody and gold-binding epitopes in directionally orientated untensioned microfibrils (figure 5*b*) and mapped bead and interbead mass changes on extension (figure 6). Together, these data provide compelling evidence that, whereas in extended configurations fibrillin molecules are strung out in head-to-tail arrays, in the untensioned state the molecules clearly adopt a complex folded arrangement. Such folding, perhaps driven by favourable hydrophobic and electrostatic interactions, could form the molecular engine of microfibril extensibility.

The data, summarized below, formed the basis of a new model of fibrillin alignment that is consistent with observed microfibril ultrastructure, indicates that fibrillin polymers undergo conformational maturation to a reversibly extensible beaded polymer and provides a molecular explanation of microfibril extensibility. Our model (see figure 6 and § 4c) predicts maturation from a parallel head-to-tail alignment to an approximate one-third stagger (figure 6), accounts for observed structural features, suggests that intramolecular interactions drive conformation changes to form extensible microfibrils and predicts that there are eight molecules in cross-section.

(a) *Untensioned microfibrils*

Three-dimensional reconstructions of microfibrils to 18.6 Å resolution revealed new structural features and dimensions (figure 5*a*). Beads appeared as dense masses that were more 'heart-shaped' than spherical, with undulating surfaces and resolution at domain level. Bead diameter varied axially between 14.8 and 18.7 nm. Some bead morphological variability occurred in all datasets. In most repeats, two prominent arms emerged from the broader bead face, meeting at a fixed position *ca.* 43% of bead-to-bead distance (14.7 nm from bead edge, *ca.* 29% of the interbead). They appeared as stain-excluding regions that bow out between the beads and between which there is a stain-accessible space. In some repeats, the arms were less clearly defined, appearing as a number of fine filaments. The point where the arms terminated within the interbead probably corresponded to an interbead 'striation' detected by rotary shadowing. The remaining interbead had a much less open structure, was generally narrower than the bead and the arms, extended for the remaining 71% of the interbead region then merged into the following bead. The repeating units often looked symmetrical about the longitudinal axis of the microfibril, although some sample variability and noise were apparent. Twisting along isolated microfibrils within the interbead may occur. In many repeats, the two interbead arms appeared to cross over between consecutive beads, which emphasized stain pooling between them and gave a 'bow-tie' appearance. Twisting supports the concept that the isolated microfibrils are in an untensioned, relaxed conformation.

Antibody binding studies on isolated microfibrils have been successful in locating fibrillin epitopes as clues to the alignment of fibrillin molecules within a microfibril. A study of the binding sites of three monoclonal anti-fibrillin-1 antibodies on partially extended microfibrils showed that N- and C-terminal epitopes were positioned on either side of the bead and suggested that fibrillin molecules were assembled in a head-to-tail arrangement (Reinhardt *et al.* 1996*b*). More recently, we mapped the epitopes of four fibrillin-1 antibodies accessible on native untensioned microfibrils (figure 5*b*) (Baldock *et al.* 2001). The binding site for monoclonal antibody 2052, which recognizes an N-terminal fibrillin-1 sequence within residues 45–450, was close to the bead on the side opposite the arms (15.9% of bead-to-bead distance). Monoclonal antibody 11C1.3 (epitope within fibrillin-1 residues 654–909) bound to microfibrils at the interbead striation where the arms terminate. Incubation with this antibody generated numerous extensive parallel microfibril arrays with beads in-register and the antibody binding at 41.1% of bead-to-bead distance. PF2 polyclonal antibody, which recognizes pepsin fragment PF2 (Maddox *et al.* 1989) (sequences encoded by exons 41–45), bound close to the centre of the interbead (47.1% or 52.9% of bead-to-bead distance). The binding site for monoclonal antibody 2499, which recognizes a C-terminal fibrillin-1 sequence within residues 2093–2732 (assuming furin cleavage), was on the arms close to the bead (20.2% of bead-to-bead distance).

(b) *Extended microfibrils*

Several experimental approaches have been investigated in order to extend microfibrils *in vitro* (Baldock *et al.* 2001). When microfibril preparations were centrifuged at 60 000 *g* for 1 h, a small proportion of microfibrils appeared extended in the range 70–110 nm, but most retained untensioned periodicity. When microfibril preparations were repeatedly drawn through narrow bore needles, the majority of microfibrils retained untensioned (*ca.* 56 nm) periodicity, although a few were extended to *ca.* 70 nm. Surface-tensional forces did provide a means of trapping many microfibrils in an extended state (also 70–110 nm) directly from sample drop surfaces onto carbon-coated grids; the interbead morphology of these microfibrils often appeared diffuse, suggesting major conformational changes (Baldock *et al.* 2001). In addition, when antibody-treated (11C1.3) human microfibrils were extended in this way, antibody-banded microfibril arrays were detected that were partially extended to *ca.* 70 nm, with the antibody position remaining at the end of the interbead arms (23 nm from bead centre). This corresponds to 41.1% of bead-to-bead distance for untensioned 56 nm microfibrils, but 32% of bead-to-bead distance for 70 nm microfibrils. Thus, microfibrils can extend at least 10 nm before this epitope has to move. At higher extensions, all antibody banding was lost.

Colloidal gold particles bind proteins through charge, hydrophobic interaction or dative binding to sulphur-containing groups (Hermanson 1996). They associate periodically, and often pairwise, with untensioned microfibrils at the ends of the interbead arms, but on extended microfibrils the gold bound periodically only at the beads, confirming major molecular rearrangements on extension (Baldock *et al.* 2001).

Unstretched (*ca.* 56 nm) and extended microfibrils isolated from canine zonules were examined by STEM to investigate how mass distribution changes on extension (Baldock *et al.* 2001). Within any single microfibril, many

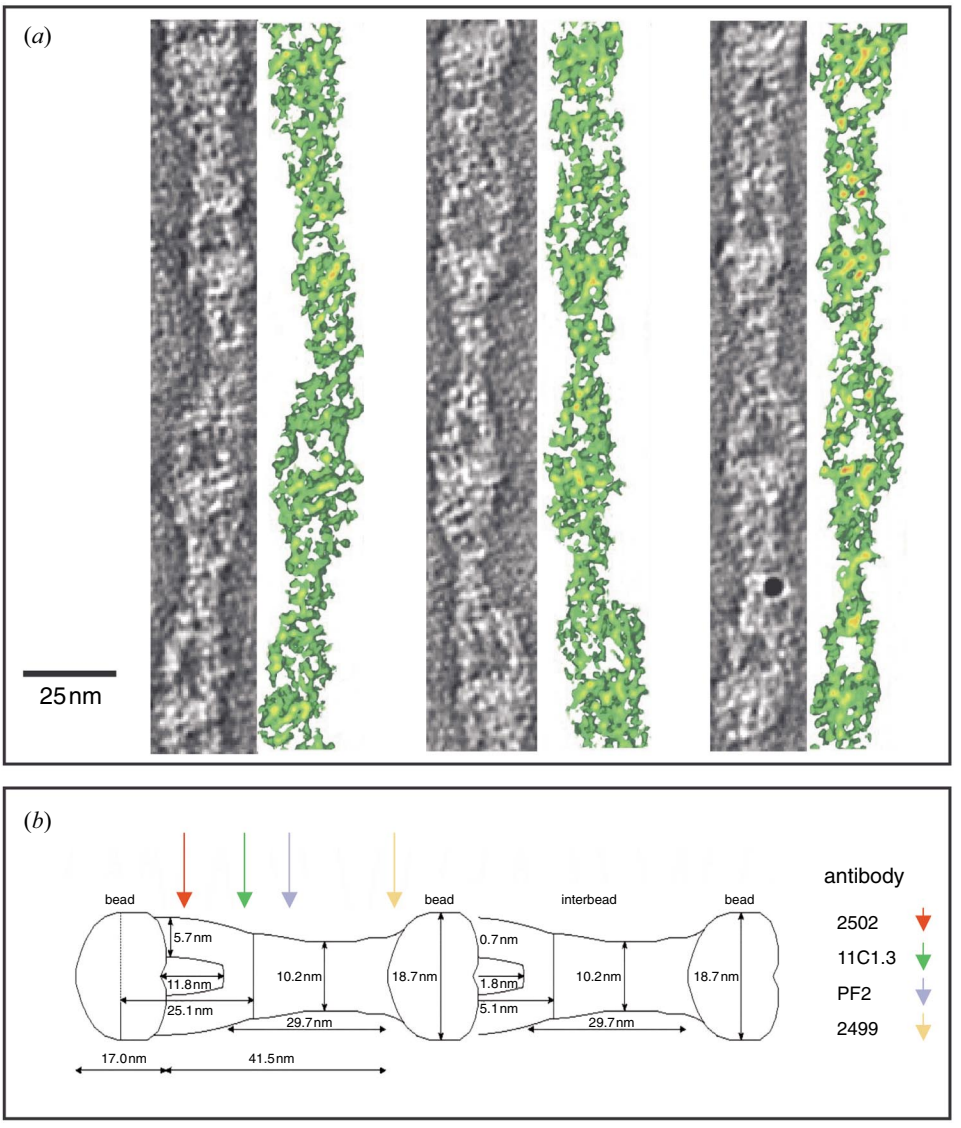

Figure 5. AET images of negatively-stained untensioned bovine zonular microfibrils. (*a*) Three Z-slices shown in black and white compared with the same region of microfibril 3D rendered (green) using AVS Express (Advanced Visual Systems Inc., 300 Fifth Avenue, Waltham, MA 02451, USA). Scale bar, 25 nm. (*b*) Schematic diagram of a two-microfibril repeating unit with the mean measurements taken from a representative dataset. The binding positions of four anti-fibrillin-1 antibodies are shown with coloured arrows (Baldock *et al.* 2001). Reproduced with permission from Rockefeller Press, USA.

repeats were *ca.* 56 nm, but at stretched regions, there was always a sharp periodicity transition from under 95 nm to over 110 nm (figure 7). Total mass per repeat remained unchanged irrespective of microfibril periodicity, but there was a progressive reduction in interbead MUL and loss of the shoulder at periodicities from *ca.* 56 to 100 nm, then a rapid reduction in bead mass at higher periodicities. This is evidence that interbead unfolding accounts for extension between *ca.* 56 and 100 nm and that bead unravelling occurs at periodicities above 100 nm. Interestingly, such highly extended arrays appear to be irreversibly stretched since they are stable in solution.

(c) *Molecular alignment and reversible extensibility*

(i) We have proposed that the first step in microfibril assembly is N- and C-terminal association at the cell surface, perhaps regulated by terminal processing (figure 6). This would generate linear head-to-tail polymers with a repeating periodicity corresponding to a molecular length of *ca.* 160 nm.

(ii) Molecular association between internal sequences (within exons 12–15 and 50–64, after processing) driven by folding at the termini and proline-rich region, would reconfigure consecutive molecules into an approximate one-third stagger with N- and C-terminal sequences 'looped out' (figure 6). This association would align fibrillin-1 transglutaminase cross-link sequences (exons 14–16 and 56–58) and allow cross-link stabilization of this folded arrangement. The repeating periodic distance of these polymers would be *ca.* 100 nm (32 cbEGFs, 1 hybrid motif, 5 TB modules) and the 'looped out' termini could contribute to the beads. This arrangement may provide the structural context for reversible extension between *ca.* 100 nm and a more energetically stable 56 nm.

(iii) Microfibril 'recoil' could involve intramolecular

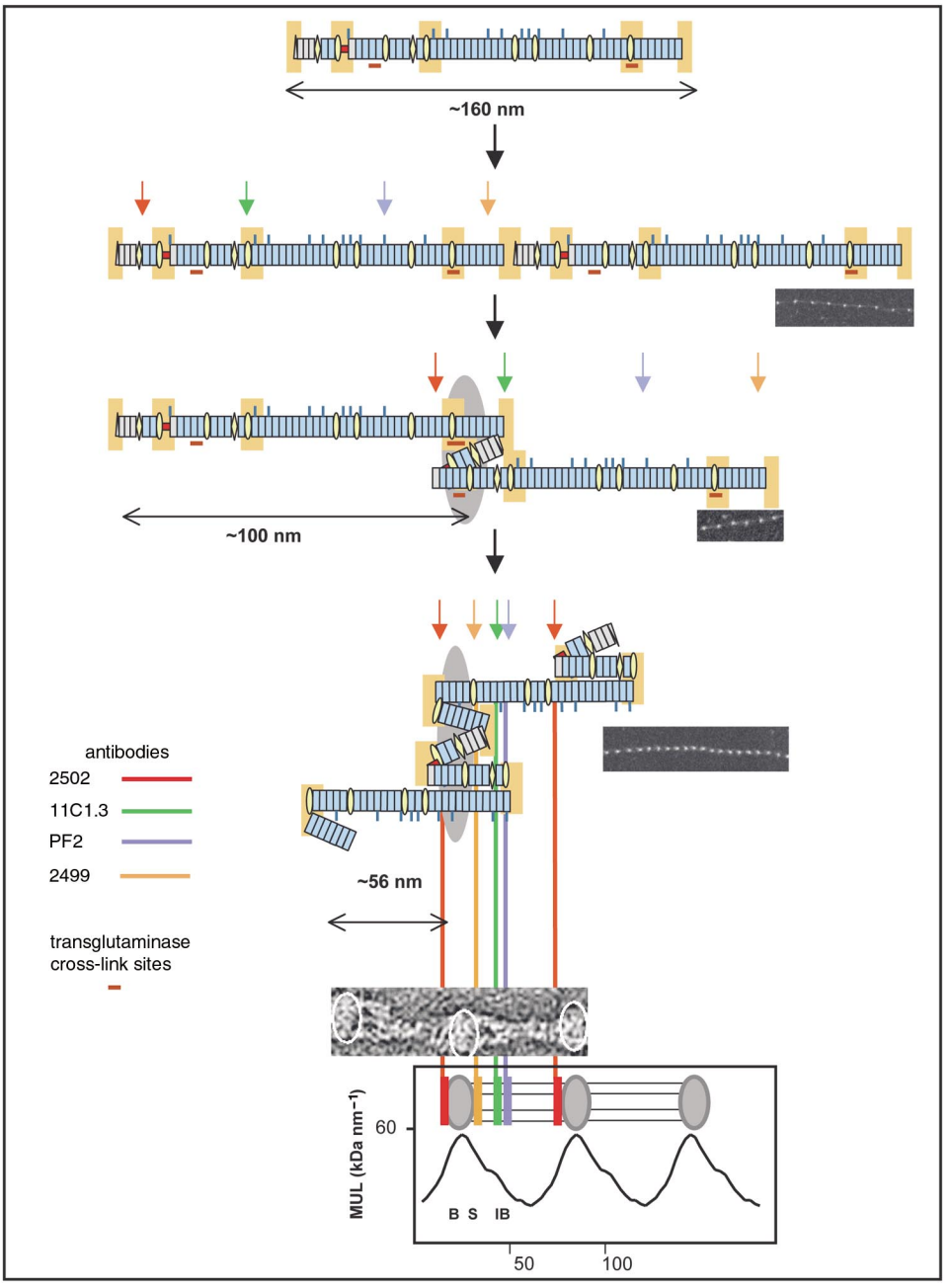

Figure 6. A model of fibrillin alignment in microfibrils. Schematic diagram depicting a possible folding arrangement of fibrillin molecules in a beaded microfibril. Two N- and C-terminally processed molecules associate head-to-tail to give *ca.* 160 nm periodicity. Subsequent molecular folding events could generate *ca.* 100 nm periodicity, then *ca.* 56 nm periodicity. The model is supported by AET, STEM data, antibody localizations and microfibril extension studies (Baldock *et al.* 2001). Whilst the predicted fold sites are shown (orange boxes), it should be noted that the precise packing arrangement of folded segments contributing to the bead remains unresolved. The inset shows STEM images of microfibrils with periodicities corresponding to those predicted. Observed antibody binding sites are overlaid on the *ca.* 56 nm periodic folding arrangement. The axial mass distribution of *ca.* 56 nm microfibrils (shown at the bottom of the figure) correlates well with the corresponding predicted molecular folding.

folding at potentially flexible TB–cbEGF linkages (Yuan *et al.* 1997, 1998) (calcium-bound cbEGF arrays form rod-like arrays) (figure 6). As five TB–cbEGF junctions exist between the cross-link sites, a number of potential folding arrangements could be adopted in untensioned microfibrils. However, two lines of evidence suggest that major hinging may occur at the TB3–cbEGF junction such that the central 12 cbEGF array folds back, juxtaposing the centre of this array with the core bead, thereby enhancing its mass and reducing periodicity to *ca.* 56 nm (18 cbEGFs, 3 TB modules). TB3, which precedes the central 12-cbEGF array, has the longest linker region (19 residues) and may be particularly flexible. More specifically, only this folding arrangement fits the observed antibody binding pattern and formation of interbead arms of observed dimensions (14.7 nm or approximately six domains).

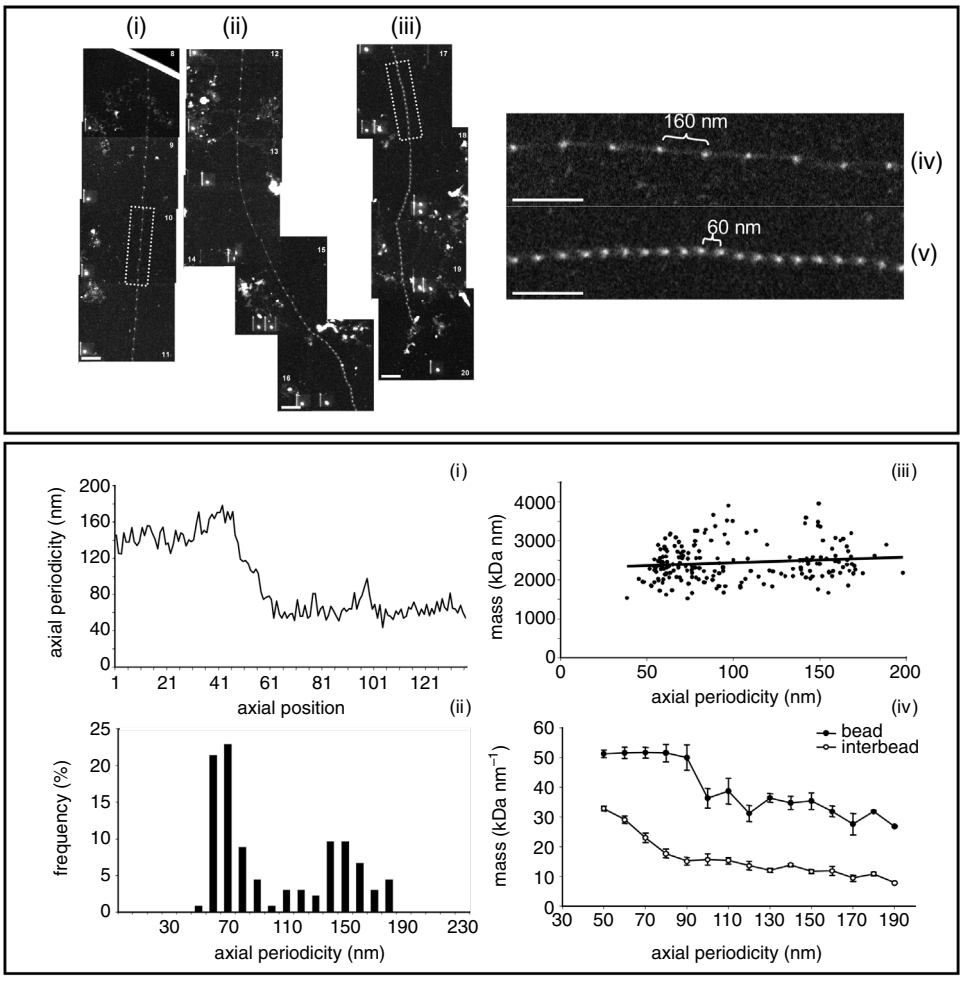

Figure 7. STEM mass mapping of untensioned and stretched microfibrils. (*a*) Dark-field STEM composite of a highly stretched fibrillin-rich microfibril isolated from canine zonules (i, ii and iii). High magnification (iv, v) of regions indicated by boxes in (i) and (iii). Microfibril periodicity varied between 160 nm (iv) and 56 nm (v), with a short sharp transition zone. Scale bars, 200 nm. (*b*) Analysis of microfibril mass and its distribution in untensioned and extended microfibril regions. (i, ii) Bead-to-bead periodicity showing a sharp transition from untensioned to extended state. (iii) Total mass per repeat (kDa) was invariant with changes in periodicity. (iv) Central bead and central interbead mass measurements. Interbead mass falls as periodicity increases from *ca.* 56 nm to *ca.* 100 nm, but bead mass remains constant until *ca.* 90–100 nm then falls rapidly. Periodicities between *ca.* 56 and 100 nm may be reversible, whereas those greater than *ca.* 100 nm may be irreversible (Baldock *et al.* 2001). Filled circles represent bead and open circles interbead. Reproduced, with permission, from Rockefeller Press, USA.

N-glycosylation sites would be accommodated within the interbead, where they could protect exposed interbead domain arrays from proteolytic attack.

(iv) Reversible extension (*ca.* 56–100 nm) would involve unfolding of the TB3–cbEGF fold. Irreversible extension (more than 100 nm) would involve disruption of the molecular association at the transglutaminase cross-link site.

In summary, this model predicts a 'modular' elongation mechanism for the fibrillin-rich microfibrils, based on the formation and opening of defined folds. A precedent for a broadly similar mechanism exists for the adhesive fibres between the calcium carbonate plates in abalone shell (Smith *et al.* 1999). These fibres elongate in a stepwise manner as folded domains or loops are pulled open. The elongation events occur for forces of a few hundred picoNewtons, which are smaller than the forces of greater than 1 nN required to break the polymer backbone in the threads. This general mechanism could well prove to be a relatively common means of conveying toughness and elasticity to natural fibres and adhesives.

(d) *Number of fibrillin molecules in cross-section*

The AET and STEM data (figures 5 and 7) both predict that there are approximately eight fibrillin molecules in a microfibril cross-sectional diameter. The reconstructions of untensioned microfibrils contain volumetric information indicating how many linearly aligned fibrillin molecules are packed within the interbead. The arms emerging from the bead each measure *ca.* 6×5 nm (30 nm^2) in cross-section. Because the cross-sectional diameter of calcium-bound cbEGF-like domains, as determined by NMR (Downing *et al.* 1996), is *ca.* 3.6 nm^2, this corresponds to approximately eight domain arrays per arm. In our model, since each molecule in the arms is folded back, there would be four molecules per

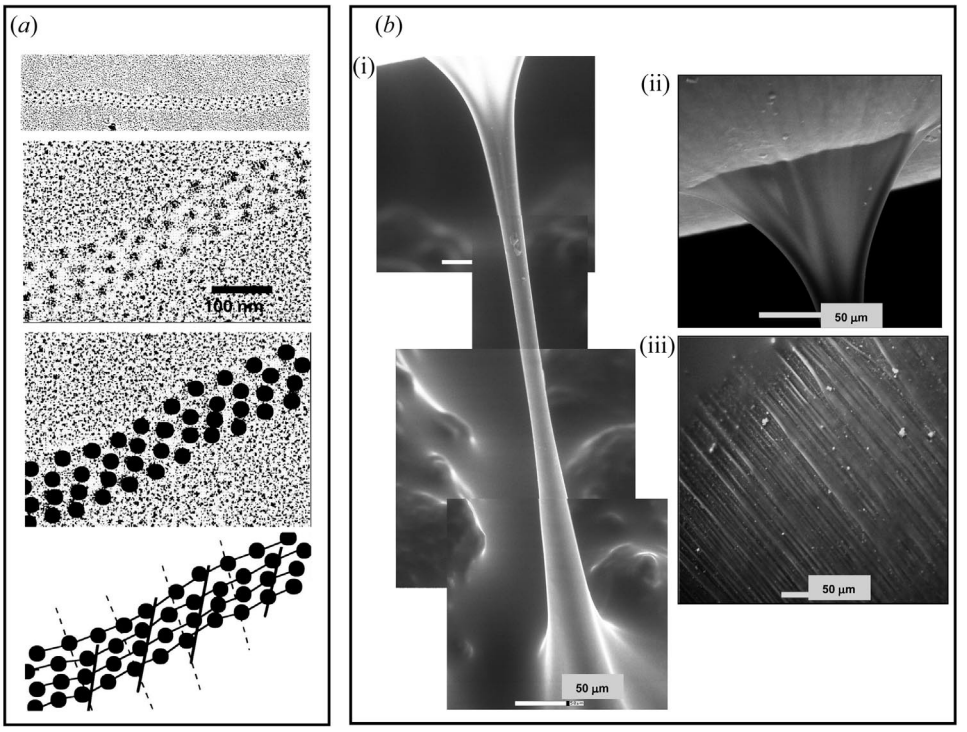

Figure 8. Ciliary zonular microfibrillar arrays. (*a*) An electron micrograph of a native microfibrillar array isolated from nuchal ligament in the presence of Ca^{2+}. Together with published X-ray diffraction studies (Wess *et al.* 1998*a*), these observations suggest that 'supramicrofibrillar junctions' may occur in zonules and in microfibril bundles in other tissues. Such juxtaposed regions may influence transmission of force through bundles. Reproduced with permission from Rockefeller Press, USA. Scale bar, 100 nm. (*b*) ESEM of the anterior (i) and posterior (ii, iii) aspects of human zonules running from the ciliary process to the lens capsule in a 68 yr old male. The length of the individual zonular fibre in (i) is *ca.* 600 μm. Insertion of the zonule into the lens capsule is shown in (ii). Scale bars, 50 nm.

arm, possibly arranged as dimer pairs or tetramers. The cross-sectional diameter of the narrow interbead region measures a minimum of *ca.* 10×6 nm (60 nm^2), so approximately 16 cbEGF domain arrays, at least, may be aligned within this region, which is consistent with predicted domain array folding. STEM has also established here that the MUL of the extended interbead is 14.25 kDa nm^{-1}. Determination of the MUL of a fibrillin molecule was based on exons 23–36 (13 cbEGF domains and a TB module). The predicted mass of this peptide is 67.18 kDa. Its length is 37.4 nm, based on domain dimensions (37.8 nm) determined by NMR (Downing *et al.* 1996; Yuan *et al.* 1997, 1998) and published measurements (35.4 and 38.3 nm; average 36.9 nm; Reinhardt *et al.* (1996*b*, 2000)). Thus, the MUL of each molecule is *ca.* 1.80 kDa nm^{-1}, which indicates 7.92 molecules in an extended interbead cross-section. Moreover, the actual mass per repeat is *ca.* 2490–2510 kDa compared with a predicted 2510 kDa for eight aligned molecules.

(e) *Microfibril bundle extensibility and organization*

Following this in-depth consideration of the packing and extensibility of individual microfibrils, it is important to bear in mind that the *in vivo* arrangement of microfibrils in bundles and in elastic fibres will profoundly influence the ability of individual microfibrils, within such higher-order arrays, to extend and retract. X-ray fibre diffraction has proved to be a useful experimental tool for investigating microfibril arrays (figure 8) (Wess *et al.* 1997, 1998*a*,*b*). The X-ray diffraction of microfibrils in the form of hydrated bovine zonular filaments exhibited meridional diffraction peaks indexing on a fundamental periodicity of *ca.* 56 nm in the relaxed state (Wess *et al.* 1997). These arrays are capable of reversible extension within a defined extension range (up to *ca.* 50%). However, when zonules were stretched beyond this range, there was extensive deterioration in the quality of diffraction and the microfibril bundles were no longer reversibly extensible (Wess *et al.* 1998*b*). Microfibril extensibility was shown to be independent of the presence or absence of calcium, although the starting periodicities of the microfibrils was different (*ca.* 56 versus 39 nm), in line with similar observations made by STEM and rotary shadowing on isolated microfibrils (Wess *et al.* 1998*a*). Interestingly, the periodicity of a small proportion of microfibrils always remained unchanged on bundle extension, leading to the prediction that one-third (0.33-D) staggered microfibril 'junction' arrays exist within discrete regions of zonular bundles that may be important in modulating force transmission within the microfibril bundle.

5. SUMMARY AND FUTURE PERSPECTIVES

The unique fibrillin-rich microfibrils of the extracellular matrix have been shown to play an essential role in the provision of long-range extensibility to many dynamic connective tissues. Recent details of their structure and assembly have begun to reveal precisely how these microfibrils are assembled and the molecular basis of their

unique biomechanical properties. Despite this recent progress, many questions remain unanswered. What is the precise molecular composition of microfibrils in different tissues? How is intracellular assembly regulated and limited? What controls the number of molecules in cross-section? Are fibrillin molecules flexible? What intra- and intermolecular forces and interactions drive extension and recoil? What intermolecular cross-links stabilize microfibrils? Another interesting question has recently arisen: is there more than one form of fibrillin polymer? This possibility was suggested by immunofluorescence studies on human dermal fibroblast cultures, in which one anti fibrillin-1 antibody did not detect extracellular microfibrils until almost two weeks in culture, whereas a second antibody detected abundant extensive fibrillin-1 microfibrils within three days (Baldock *et al.* 2001). One explanation for this observation could be that conformational changes occur during maturation of beaded microfibrils that expose or unmask cryptic epitopes; such structural changes could correspond to conversion from head-to-tail fibrillin arrays to mature, approximately one-third staggered, beaded microfibrils. Future studies will undoubtedly focus on defining the molecular motor that drives microfibril extension and recoil, and on establishing how these unique extensible properties can be modified by interactions with other matrix molecules and by incorporation into microfibril bundles.

C.M.K. (with C.B. and M.J.R.) is funded by the Medical Research Council.

REFERENCES

Ashworth, J. L., Murphy, G., Rock, M. J., Sherratt, M. J., Shapiro, S. D., Shuttleworth, C. A. & Kielty, C. M. 1999*a* Fibrillin degradation by matrix metalloproteinases: implications for connective tissue remodelling. *Biochem. J.* **340**, 171–181.

Ashworth, J. L., Kelly, V., Wilson, R., Shuttleworth, C. A. & Kielty, C. M. 1999*b* Fibrillin assembly: dimer formation mediated by amino-terminal sequences. *J. Cell Sci.* **112**, 3549–3558.

Ashworth, J. L., Kelly, V., Rock, M. J., Shuttleworth, C. A. & Kielty, C. M. 1999*c* Regulation of fibrillin carboxy-terminal furin processing by N-glycosylation, and association of amino- and carboxy-terminal sequences. *J. Cell Sci.* **112**, 4163–4171.

Ashworth, J. L., Kielty, C. M. & McLeod, D. 2000 Fibrillin and the eye. *Br. J. Ophthalmol.* **84**, 1312–1317.

Baldock, C., Koster, A. J., Ziese, U., Sherratt, M. J., Kadler, K. E., Shuttleworth, C. A. & Kielty, C. M. 2001 The supramolecular organisation of fibrillin-rich microfibrils. *J. Cell Biol.* **152**, 1045–1056.

Cardy, C. M. & Handford, P. A. 1998 Metal ion dependency of microfibrils supports a rod-like conformation for fibrillin-1 calcium-binding epidermal growth factor-like domains. *J. Mol. Biol.* **276**, 855–860.

Cleary, E. G. & Gibson, M. A. 1983 Elastin-associated microfibrils and microfibrillar proteins. In *International review of connective tissue research*, vol. 10 (ed. D. A. Hall & D. S. Jackson), pp. 97–209. London: Academic.

Dallas, S. L., Keene, D. R., Bruder, S. P., Saharinen, J., Sakai, L. Y., Mundy, G. R. & Bonewald, L. F. 2000 Role of the latent transforming growth factor beta binding protein 1 in fibrillin-containing microfibrils in bone cells *in vitro* and *in vivo*. *J. Bone Miner. Res.* **15**, 68–81.

Doliana, R., Mongiat, M., Bucciotti, F., Giacomello, E., Deutzmann, R., Volpin, D., Bressan, G. M. & Colombatti, A. 1999 Emilin, a component of the elastic fiber and a new member of the C1q/tumor necrosis factor superfamily of proteins. *J. Biol. Chem.* **374**, 16 773–16 781.

Downing, A. K., Knott, V., Werner, J. M., Cardy, C. M., Campbell, I. D. & Handford, P. A. 1996 Solution structure of a pair of calcium binding epidermal growth factor-like domains: implications for the Marfan syndrome and other genetic disorders. *Cell* **85**, 597–605.

Fleischmajer, R., Perlish, J. S. & Faraggiana, T. 1991 Rotary shadowing of collagen monomers, oligomers and fibrils during tendon fibrillogenesis. *J. Histochem. Cytochem.* **39**, 51–58.

Handford, P. A., Downing, A. K., Reinhardt, D. P. & Sakai, L. Y. 2000 Fibrillin: from domain structure to supramolecular assembly. *Matrix Biol.* **19**, 457–470.

Hermanson, G. T. 1996 Preparation of colloidal-gold-labelled proteins. In *Bioconjugate techniques*, pp. 593–604. San Diego: Academic.

Keene, D. R., Maddox, B. K., Kuo, H. J., Sakai, L. Y. & Glanville, R. W. 1991 Extraction of beaded structures and their identification as fibrillin-containing matrix microfibrils. *J. Histochem. Cytochem.* **39**, 441–449.

Kielty, C. M. & Shuttleworth, C. A. 1993 The role of calcium in the organisation of fibrillin microfibrils. *Federation European Biol. Sci. Lett.* **336**, 323–326.

Kielty, C. M. & Shuttleworth, C. A. 1995 Fibrillin-containing microfibrils—structure and function in health and disease. *Int. J. Biochem. Cell Biol.* **27**, 747–760.

Kielty, C. M., Cummings, C., Whittaker, S. P., Shuttleworth, C. A. & Grant, M. E. 1991 Isolation and ultrastructural analysis of microfibrillar structures from foetal bovine elastic tissues. Relative abundance and supramolecular architecture of type VI collagen assemblies and fibrillin. *J. Cell Sci.* **99**, 797–807.

Kielty, C. M., Whittaker, S. P. & Shuttleworth, C. A. 1996 Fibrillin: evidence that chondroitin sulphate proteoglycans are components of microfibrils and associate with newly synthesised monomers. *Federation European Biol. Sci. Lett.* **386**, 169–173.

Lee, B. L., Godfrey, M., Vitale, E., Hori, H., Mattei, M.-G., Sarfarazi, M., Tsipouras, P., Ramirez, F. & Hollister, D. W. 1991 Linkage of Marfan syndrome and a phenotypically related disease to two different genes. *Nature* **352**, 330–334.

Lee, D., Rock, M. J., Phillips, S., Shuttleworth, C. A. & Kielty, C. M. 2001 Assembly of full-length and minigene recombinant fibrillin-1 (Submitted.)

McConnell, C. J., Wright, G. M. & DeMont, M. E. 1996 The modulus of elasticity of lobster aorta microfibrils. *Experientia* **52**, 918–921.

Maddox, B. K., Sakai, L. R., Keene, D. R. & Glanville, R. W. 1989 Connective tissue microfibrils: isolation and characterization of three large pepsin-resistant domains of fibrillin. *J. Biol. Chem.* **264**, 21 381–21 385.

Maslen, C. L., Corson, G. M., Maddox, B. K., Glanville, R. W. & Sakai, L. Y. 1991 Partial sequence of a candidate gene for the Marfan syndrome. *Nature* **352**, 334–337.

Mecham, R. P. & Heuser, J. E. 1991 The elastic fiber. In *Cell biology of the extracellular matrix*, 2nd edn (ed. E. D. Hay), pp. 79–109. New York: Plenum Press.

Pereira, L., D'Alessio, M., Ramirez, F., Lynch, J. R., Sykes, B., Pangilinan, T. & Bonadio, J. 1993 Genomic organization of the sequence coding for fibrillin, the defective gene product in Marfan syndrome. *Hum. Mol. Genet.* **2**, 961–968.

Qian, R. Q. & Glanville, R. W. 1997 Alignment of fibrillin molecules in elastic microfibrils is defined by transglutaminase-derived cross-links. *Biochem.* **36**, 15 841–15 847.

Raghunath, M., Tschodrich-Rotter, M., Sasaki, T., Meuli, M.,

Chu, M. L. & Timpl, R. 1999*a* Confocal laser scanning analysis of the association of fibulin-2 with fibrillin-1 and fibronectin define different stages of skin regeneration. *J. Invest. Dermatol.* **112**, 97–101.

Raghunath, M., Putnam, E. A., Ritty, T., Hamstra, D., Park, E. S., Tschodrich-Rotter, M., Peters, R., Rehemtulla, A. & Milewicz, D. M. 1999*b* Carboxy-terminal conversion of profibrillin to fibrillin at a basic site by PACE/furin-like activity required for incorporation in the matrix. *J. Cell Sci.* **112**, 1093–1100.

Reinhardt, D. P., Sasaki, T., Dzamba, B. J., Keene, D. R., Chu, M. L., Göhring, W., Timpl, R. & Sakai, L. Y. 1996*a* Fibrillin-1 and fibulin-2 interact and are colocalized in some tissues. *J. Biol. Chem.* **271**, 19 489–19 496.

Reinhardt, D. P., Keene, D. R., Corson, G. M., Pöschl, E., Bächinger, H. P., Gambee, J. M. & Sakai, L. Y. 1996*b* Fibrillin-1: organisation in microfibrils and structural properties. *J. Mol. Biol.* **258**, 104–116.

Reinhardt, D. P., Mechling, D. E., Boswell, B. A., Keene, D. R., Sakai, L. Y. & Bächinger, H. P. 1997 Calcium determines the shape of fibrillin. *J. Biol. Chem.* **272**, 7368–7373.

Reinhardt, D. P., Gambee, J. E., Ono, R. N., Bächinger, H. P. & Sakai, L. Y. 2000 Initial steps in assembly of microfibrils. Formation of disulphide bonded cross-linked multimers containing fibrillin-1. *J. Biol. Chem.* **275**, 2205–2210.

Ren, Z. X., Brewton, R. G. & Mayne, R. 1991 An analysis by rotary shadowing of the structure of the mammalian vitreous humor and zonular apparatus. *J. Struct. Biol.* **106**, 57–63.

Ritty, T. M., Broekelmann, T., Tisdale, C., Milewicz, D. M. & Mecham, R. P. 1999 Processing of the fibrillin-1 carboxyl-terminal domain. *J. Biol. Chem.* **274**, 8933–8940.

Ritty, T. M., Broekelmann, T. J. & Mecham, R. P. 2000 Fibrillin 1 contains a proteolytically activated heparin binding site important for extracellular matrix deposition. *Mol. Biol. Cell* **11**, S1377.

Robinson, P. N. & Godfrey, M. 2000 The molecular genetics of Marfan syndrome and related microfibrillopathies. *J. Med. Genet.* **37**, 9–25.

Sakai, L. Y., Keene, D. R. & Engvall, E. 1986 Fibrillin, a new 350-kd glycoprotein, is a component of extracellular microfibrils. *J. Cell Biol.* **103**, 2499–2509.

Sherratt, M. J., Holmes, D. F., Shuttleworth, C. A. & Kielty, C. M. 1997 Scanning transmission electron microscopy mass analysis of fibrillin-containing microfibrils from foetal elastic tissues. *Int. J. Biochem. Cell Biol.* **29**, 1063–1070.

Sherratt, M. J., Wess, T. J., Baldock, C., Ashworth, J., Purslow, P. P., Shuttleworth, C. A. & Kielty, C. M. 2000 Fibrillin-rich microfibrils of the extracellular matrix: ultrastructure and assembly. *Micron* **32**, 185–200.

Sinha, S., Nevett, C., Shuttleworth, C. A. & Kielty, C. M. 1998 Cellular and extracellular biology of the latent transforming growth factor-beta binding proteins. *Matrix Biol.* **17**, 529–545.

Smith, B. L., Schaffer, T. E., Viani, M., Thompson, J. B., Frederick, N. A., Kindt, J., Belcher, A., Stucky, G. D., Morse, D. E. & Hansma, P. K. 1999 Molecular mechanistic origin of the toughness of natural adhesives, fibres and composites. *Nature* **399**, 761–763.

Thurmond, F. A. & Trotter, J. A. 1996 Morphology and biomechanics of the microfibrillar network of sea cucumber dermis. *J. Exp. Biol.* **199**, 1817–1828.

Trask, T. M., Ritty, T. M., Broekelmann, T., Tisdale, C. & Mecham, R. P. 1999 N-terminal domains of fibrillin 1 and fibrillin 2 direct the formation of homodimers: a possible first step in microfibril assembly. *Biochem J.* **340**, 693–701.

Trask, B. C., Trask, T. M., Broekelmann, T. & Mecham, R. P. 2000*a* The microfibrillar proteins MAGP-1 and fibrillin-1 form a ternary complex with the chondroitin sulfate proteoglycan decorin. *Mol. Biol. Cell* **11**, 1499–1507.

Trask, T. M., Trask, B. C., Ritty, T. M., Abrams, W. R., Rosenbloom, J. & Mecham, R. P. 2000*b* Interaction of tropoelastin with the amino-terminal domains of fibrillin-1 and fibrillin-2 suggests a role for the fibrillins in elastic fiber assembly. *J. Biol. Chem.* **275**, 24 400–24 406.

Unsold, C., Hyytiainen, M., Bruckner-Tuderman, L. & Keski-Oja, J. 2001 Latent TGF-beta binding protein LTBP-1 contains three potential extracellular matrix interacting domains. *J. Cell Sci.* **114**, 187–197.

Wallace, R. N., Streeten, B. W. & Hanna, R. B. 1991 Rotary shadowing of elastic system microfibrils in the ocular zonule, vitreous and ligamentum nuchae. *Curr. Eye Res.* **10**, 99–109.

Wess, T. J., Purslow, P. & Kielty, C. M. 1997 Fibrillin-rich microfibrils: an X-ray diffraction study and elastomeric properties. *Federation European Biol. Sci. EBS Lett.* **413**, 424–428.

Wess, T. J., Purslow, P. P., Sherratt, M. J., Ashworth, J., Shuttleworth, C. A. & Kielty, C. M. 1998*a* Calcium determines the supramolecular organization of fibrillin-rich microfibrils. *J. Cell Biol.* **141**, 829–837.

Wess, T. J., Purslow, P. P. & Kielty, C. M. 1998*b* X-ray diffraction studies of fibrillin-rich microfibrils: effects of tissue extension on axial and lateral packing. *J. Struct. Biol.* **122**, 123–127.

Wright, D. W. & Mayne, R. 1988 Vitreous humor of chicken contains two fibrillar systems: an analysis of their structures. *J. Ultrastruct. Mol. Struct. Res.* **100**, 224–234.

Wright, D. M., Duance, V. C., Wess, T. J., Kielty, C. M. & Purslow, P. P. 1999 The supramolecular organisation of fibrillin-rich microfibrils determines the mechanical properties of bovine zonular filaments. *J. Exp. Biol.* **202**, 3011–3020.

Yuan, X., Downing, A. K., Knott, V. & Handford, P. A. 1997 Solution structure of the transforming growth factor beta-binding protein-like module, a domain associated with matrix fibrils. *European Mol. Biol. Org. J.* **16**, 6659–6666.

Yuan, X., Werner, J. M., Knott, V., Handford, P. A., Campbell, I. D. & Downing, K. 1998 Effects of proline *cis-trans* isomerisation on TB domain secondary structure. *Protein Sci.* **7**, 2127–2135.

Zhang, H., Apfelroth, S. D., Hu, W., Davis, E. C., Sanguineti, C., Bonadio, J., Mecham, R. P. & Ramirez, F. 1994 Structure and expression of fibrillin-2, a novel microfibrillar component preferentially located in elastic matrices. *J. Cell Biol.* **124**, 855–863.